Bioorganic & Medicinal Chemistry 21 (2013) 3808–3820

Contents lists available at SciVerse ScienceDirect

Bioorganic & Medicinal Chemistry

journal homepage: www.elsevier.com/locate/bmc

Curcumin-I Knoevenagel's condensates and their Schiff's bases as anticancer agents: Synthesis, pharmacological and simulation studies ☆

Imran Ali [a,*], Ashanul Haque [a], Kishwar Saleem [a], Ming Fa Hsieh [b]

[a] Department of Chemistry, Jamia Millia Islamia (Central University), New Delhi 110025, India
[b] Department of Biomedical Engineering, Chung Yuan Christian University 200, Chung Pei Rd., Chung Li, Taiwan

ARTICLE INFO

Article history:
Received 17 February 2013
Revised 8 April 2013
Accepted 9 April 2013
Available online 18 April 2013

Keywords:
Anticancer agents
Curcumin-I derivatives
Docking studies
DNA binding and hemolysis and cell line profiles

ABSTRACT

Pyrazolealdehydes (**4a–d**), Knoevenagel's condensates (**5a–d**) and Schiff's bases (**6a–d**) of curcumin-I were synthesized, purified and characterized. Hemolysis assays, cell line activities, DNA bindings and docking studies were carried out. These compounds were lesser hemolytic than standard drug doxorubicin. Minimum cell viability (MCF-7; wild) observed was 59% (1.0 μg/mL) whereas the DNA binding constants ranged from 1.4×10^3 to 8.1×10^5 M^{-1}. The docking energies varied from −7.30 to −13.4 kcal/mol. It has been observed that DNA-compound adducts were stabilized by three governing forces (Van der Wall's, H-bonding and electrostatic attractions). It has also been observed that compounds **4a–d** preferred to enter minor groove while **5a–d** and **6a–d** interacted with major grooves of DNA. The anticancer activities of the reported compounds might be due to their interactions with DNA. These results indicated the bright future of the reported compounds as anticancer agents.

1. Introduction

Cancer is considered as the second most lethal disease responsible for ~21% annual deaths globally.[1] Approximately, 7.6 million die every year worldwide due to cancer, which is expected to reach up to 13 million in 2030. In the developing and under developed countries lung, breast, colorectal, stomach and liver cancers are most common ones. On the other hand, lung and breast cancers among men and women are more prevalent in developed countries. About 1.63 million new cancer cases were expected to be diagnosed in US alone in 2012.[2] As per a report published in The Lancet,[3] total deaths due to cancer were 0.55 million in 2010 in India. It has been observed that nearly 23% deaths occurred due to oral cancer among men. On the other hand, the death percentages were 12.6% and 11.4% due to stomach and lung cancers in men. In women, 17.0% and 10.2% cases of cervical and breast cancers were reported. In this way, number of cancer patients is increasing at an alarming rate. Therefore, there is an urgent need to curb this menace. For this purpose, chemotherapy is the most commonly used treatment worldwide.[4] But it has several serious side effects and problems. These include promiscuity (binding to unwanted targets), lack of selectivity and effectiveness (especially at late stages). These limitations are compelling scientists to discover more safe and effective anticancer agents. Recently, Newman and Cragg,[5] emphasized the importance of natural products in cancer drug development. As per the authors, out of 175 anticancer agents (in the market as well as in clinical trials), 85 are directly derived from nature. Besides, 131 are also indirectly connected to the natural sources.[5] Some other reviews[6,7] also highlighted the importance of natural products in cancer chemotherapy. The natural products (with no or least side effects) are being exploited for developing effective anti-cancer drugs, especially, by modifying their molecular structures. Among several natural products, the active constituent of *Curcuma longa*, (curcumin) is used as precursor for developing various medicines. It is due to its fair pharmaceutical properties including anticancer.[8–10] Low pharmaceutical activities of curcumin-I are due to its low plasma concentration and poor membrane permeation. From the structure activity relationship (SAR), it has been established that two C=C bonds between 1,3-dicarbonyl and 3-methoxy, 4-hydroxyphenyl moieties on each side (Fig. 1) are important sites to enhance the pharmaceutical activities[11,12] of curcumin-I.

Several modifications, especially, at the methylene centre of curcumin-I have been reported to increase its biological activity.[13,14] Knoevenagel's condensates of curcumin-I are considered to be the effective derivatives. Qiu et al.[15] reported 4-arylidene analogues of curcumin-I, which showed better anticancer activity than native curcumin-I. Simoni et al.[16] developed isoxazole

☆ Part of this paper was presented in "*International Conference on Chemistry Frontiers and Challenges-2013*", Department of Chemistry, Aligarh Muslim University, Aligarh (UP), India.

* Corresponding author. Tel.: +91 9211458226.
E-mail addresses: drimran.chiral@gmail.com, drimran_ali@yahoo.com (I. Ali).

0968-0896/$ - see front matter © 2013 Elsevier Ltd. All rights reserved.
http://dx.doi.org/10.1016/j.bmc.2013.04.018

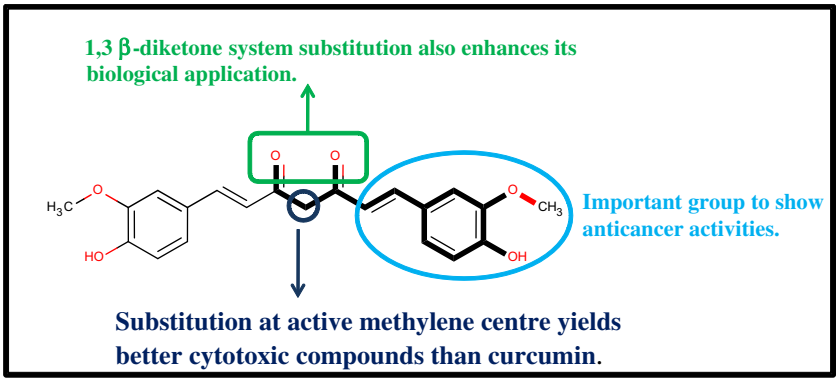

Figure 1. Important sites of the curcumin molecule responsible for its anticancer activities.

derivative of curcumin-I, which inhibited the growth of MCF-7 (MDR) human cancer cell lines moderately. Earlier, we have also reported Knoevenagel's condensates of curcumin-I and their ruthenium metal ion complexes. It was observed that the synthesized compounds had good anticancer activities for MDR-MB-231, HepG2, HeLa and HT-29 cell lines.[17] The literature survey and our own experience dictate us that the inclusion of a heterocyclic moiety increases the activity of the molecules in most of the cases. Among heterocycles, pyrazoles have gained good reputation, especially, in the field of anticancer drug development.[18–20] Figure 2 shows some of the pyrazole moieties, which are under study worldwide.[18–24]

In view of these facts, attempts have been made to incorporate pyrazolealdehyde moieties into curcumin-I via Knoevenagel's condensation. The resulting derivatives were allowed to react with semicarbazide to form disemicarbazones (Schiff's bases). The developed molecules were purified and characterized by chromatographic and spectroscopic techniques. DNA binding studies,

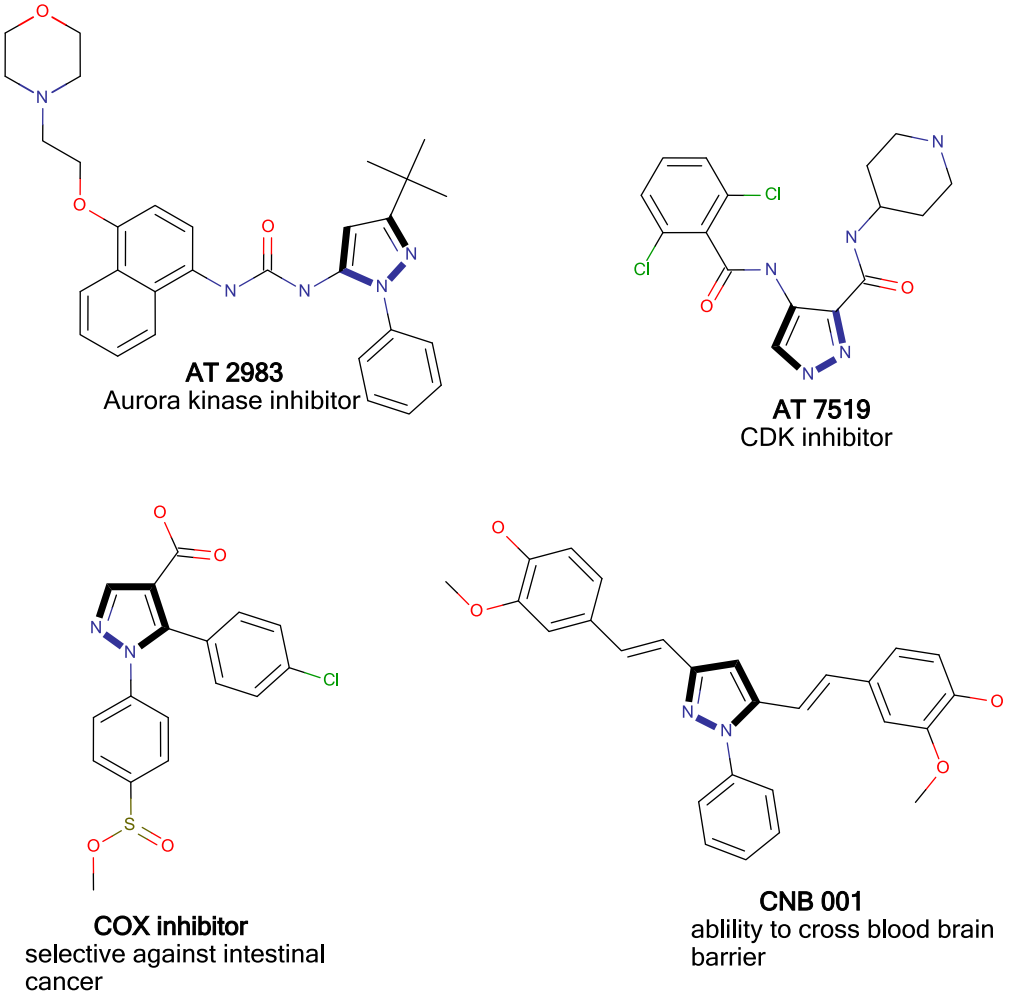

Figure 2. Structure of some pharmacologically active compounds bearing (anticancer) pyrazoles moiety.

hemolytic assays and anticancer studies on MCF-7(wild) cell line have also been carried out. In vitro DNA bindings and anticancer activities of the developed compounds have been verified by simulation studies. The efforts have also been made to develop the mechanism of action (interactions with DNA grooves) at supramolecular level using the data of above cited studies. Besides, the future perspectives of the reported compounds were also predicted. The results of these findings are discussed herein.

2. Results

2.1. Chemistry

Phenyl hydrazones were prepared by using phenyl hydrazine (**1**) *ortho*, *meta* and *para* substituted acetophenone (**2a–d**). The so formed *ortho*, *meta* and *para*-phenyl hydrazones (**3a–d**) were used to synthesize *ortho*, *meta* and *para*-substituted pyrazolealdehydes (**4a–d**) by employing Vilsmeier–Haack's reaction. Knoevenagel's condensates (**5a–d**) were prepared by the reaction of pyrazolealdehydes with curcumin-I in the presence of catalytic amount of piperidine. The final products (**6a–d**; Scheme 1) were prepared by the reaction of Knoevenagel's condensates (**5a–d**) with semicarbazide hydrochloride. These compounds were washed with petroleum ether, hexane and DCM/MeOH (99:1 v/v). Furthermore, the purities of these compounds were confirmed by recording their melting points, UV–vis spectra and elemental analyses. The structures of the synthesized compounds were determined by FT-IR, ^{1}H NMR and ESI-MS spectral studies.

2.2. Discussion

2.2.1. Characterization of the products

The products (**4a–d**) were characterized by the presence of a characteristic ^{1}H NMR signal of pyrazole protons in the range of 8.52–9.21 ppm, while aldehydic proton appeared in the range of 9.90–10.10 ppm. A strong IR stretching frequency in the region of 1690–1680 cm^{-1} was observed in compounds **4a–d**, indicating the presence of carbonyl groups. The values of ESI-MS (*m*/*z*) were found 293.94 for **4a**, 287.17 for **4b**, 316.20 for **4c** and 283.15 for **4d**; confirming the formation of pyrazolealdehydes. The formation of compounds **5a–d** via Knoevenagel's condensation was confirmed by the absence of aldehydic protons (at 10.10 ppm) and the presence of arylidene proton (=C**H**-Ar) in the range of 7.77–7.82 (s, =C**H**-Ar). It was observed that C–H stretching frequency (methylene center, both *assym.*/*symm.*) of curcumin was replaced by new conjugated –C=CH-Ar stretching frequency (1601 cm^{-1}). ESI-MS spectra of Knoevenagel's condensates (**5a–d**) showed a molecular ion peak at (*m*/*z*) 642.30 for **5a**, 633.12 for **5b**, 666.88 for **5c** and 633.21 for **5d**. These results were concrete indication of reaction completion as per Scheme 1. The resulting condensates (**5a–d**) were converted to their corresponding Schiff's bases (**6a–d**), which were characterized by the shifting of C=O frequency at 1687–1598 cm^{-1} (C=N– stretching frequency). The values of ESI-MS were found to be *m*/*z* 727.39 for **6a**, 729.29 for **6b**, 727.80 for **6c** and 748.56 for **6d**. All these spectral studies confirmed that the compounds **4a–6d** were formed as per Scheme 1.

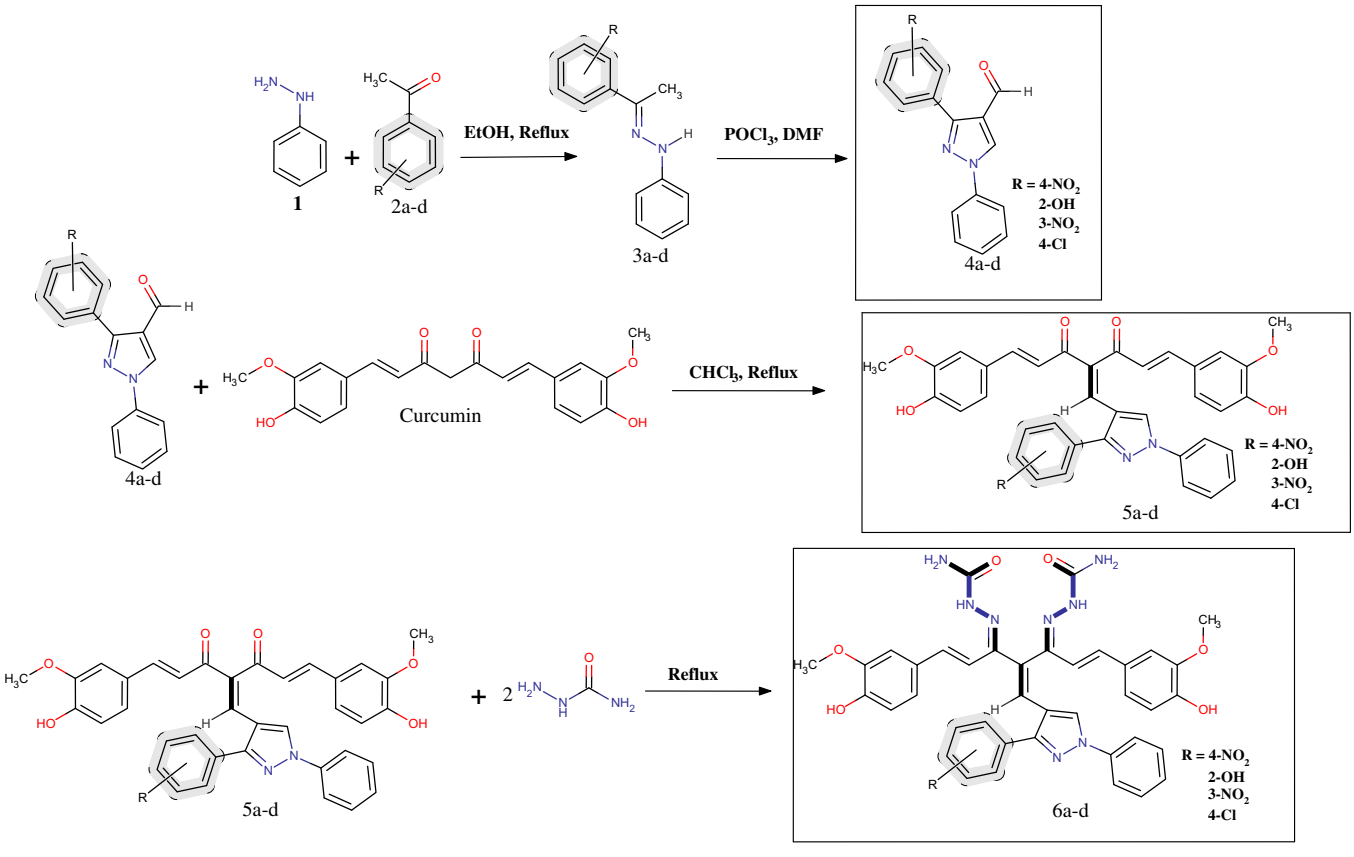

Scheme 1. Synthesis of pyrazolealdehydes (**4a–d**), curcumin based Knoevenagel condensates (**5a–d**) and their Schiff bases (**6a–d**).

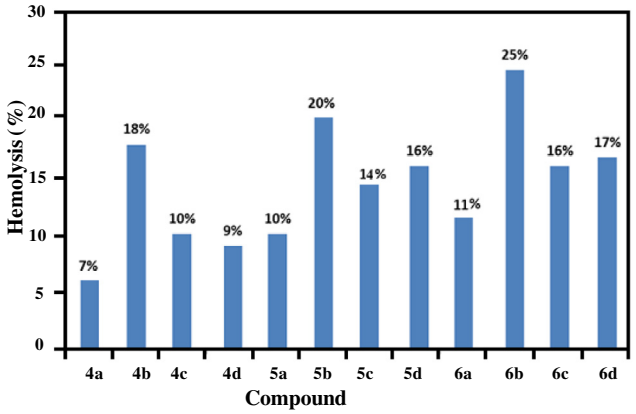

Figure 3. Hemolysis assay of the synthesized compounds on rabbit RBC.

2.3. Pharamacological activities

2.3.1. Hemolytic assay

In vitro hemolytic assay is the preliminary method to evaluate the cytotoxicity of the new compounds.[25] It is an acceptable screening tool for gauging possible in vivo toxicity to the host cells.[26] Mammalian RBCs were used to determine the toxicity of the synthesized compounds due to their freely availability and easy detection of the lyses products.

As per the standard hemolytic index (ASTM), compounds with 0–2%, 2–10%, 10–20% and 20–40% are considered as non, slightly, moderate and markedly hemolytic, respectively. On the other hand, compounds with hemolytic index above 40% are supposed as highly hemolytic in nature. The hemolytic activity of the synthesized compounds, that is, pyrazolealdehydes (**4a–d**), Knoevenagel's condensates of curcumin (**5a–d**) and their Schiff's bases (**6a–d**) are shown in Figure 3. It is clear from this figure that ⩽10%, 15%, 20% and 25% toxicities were shown by **4a**, **4c**, **4d** and **5a**; **5c** and **6a**; **4b**, **5b**, **5d**, **6c** and **6d**; **6b**, respectively, at concentration100 μg/mL. These results indicated the order of increasing toxicities as **6b > 5b > 4b > 6d > 6c = 5d > 5c > 6a = 5a > 4c > 4d > 4a**. Standard drug doxorubicin had 42% hemolysis activity at 100 μg/mL. Therefore, it may be concluded that compounds **4a**, **4c** and **4d** are slightly hemolytic, **5a**, **6a**, **5c**, **4b**, **5d**, **6c** and **6d** moderately hemolytic and **5b** and **6b** markedly hemolytic in nature.

2.3.2. DNA binding

UV–vis spectroscopy is one of the most commonly used methods for the investigation of the interactions of a compound with DNA.[27] DNA is the primary pharmacological target for many antitumor compounds. Therefore, the study of the interaction of the new compounds with DNA is quite essential to assess their anticancer activities and a possible mechanism of action. A compound can bind to DNA either via covalent (in which a labile ligand is replaced with a nitrogen atom of DNA base, such as N^7 of guanine) or non-covalent (such as intercalative, electrostatic and groove binding) interaction. Normally, a compound bound to DNA through intercalation results in hypochromism (decrease in absorbance) and bathochromism (red shift). It is due to the fact that intercalative mode involves a strong stacking interaction between aromatic chromophore and the base pairs of DNA.[28] It is believed that the extent of hypochromism depends on the strength of intercalation.[29–32] Generally, electrostatic interaction of a compound with DNA shows lower hypochromicity with no bathochromic shift[33] (due to decrease of the $\pi \rightarrow \pi^*$ transition energy as π^* orbital of the intercalated ligand couples with the orbital of the base pairs). On the other hand, a compound bound to DNA through covalent binding results in hyperchromism and red shift owing to breakage of secondary structure of DNA. The occurrence of red shift indicated the coordination of a compound with DNA through N^7 position of guanine.[34] Overall, the outside groove binding is characterized by no or minor change in UV–vis spectra; occasionally with some hyperchromicity. Contrarily, outside binding with self-stacking shows quite similar characteristics as the intercalative binding mode but to a lesser extent.[35–37] The absorption spectra of compounds **4a–6d** in the absence and presence of DNA are shown in Figure FS1 (a–l) (Supplementary data). The absorption spectra of compounds exhibited peaks in the range of 200–500 nm. The compounds of series **4a–d** had one absorption band in the range of 251–266 nm, while compounds of series **5a–d** and **6a–d** showed two bands (Supplementary data, Table TS1). In series **5a–d**, first and second bands ranged from 261 to 275 nm and 355 to 380 nm. Similarly, in series **6a–d** first and second bands appeared at 265–370 nm and 350–450 nm, respectively (Supplementary data, Table TS1). The band shifting was observed in the region of 200–450 nm by the addition of DNA. Small shifting of second band of the compounds of series **6a–d** was due to intra ligand $\pi \rightarrow \pi^*$ transitions.[38,39] The compounds with different substituent's showed different absorption bands, that is, ~248–275 nm for **4a–d** (273 nm for **4a**, 258 nm for **4b**, 256 nm for **4c** and 248 nm for **4d**). For compounds **5a–6d**, two absorptions peaks were observed, one around 250–260 nm (for **5a–d**) and another in the region of 350–450 nm (for **6a–d**). These data indicated bathochromic shift of all the compounds due to the interactions with DNA. It was also observed that with the addition of different concentrations of DNA [$0.4–1.2 \times 10^{-4}$ M], the absorption peaks underwent hyper- and hypo-chromicities for compounds (**4a–6d**) (Fig. FS1, Supplementary data), thus, indicating the formation of DNA-compound adducts.[35] Furthermore, it is interesting to note that in all the cases, hyper and hypochromic effects were observed with varying concentrations of DNA, which might be due to different types of bonding (covalent and non-covalent).[36] The hyperchromic shift at higher concentration of the bands might be due to the uncoiling of DNA (more bases embedding in DNA exposed).[40] UV–vis data for compounds **4a–6d** are given in Table 1 and Table TS1 (Supplementary data). More than one type of DNA-compound interactions have been formed (partial intercalation + electrostatic attraction) as indicated by the absence of any fixed isobestic points in titration experiment.

For a ready reference, the absorption spectra of first compound (**4a**, **5a** and **6a**; 2.0×10^{-4} M) of all three series; in both absence and presence ($0.4–1.2 \times 10^{-4}$ M) of calf-thymus DNA; are given in Figure 4a–c. The values of DNA binding constants of these compounds varied from 1.4×10^3 to 8.1×10^5 M^{-1}, indicating good interaction with DNA. The regression analysis was carried out

Table 1
UV–vis spectral data of the compounds **4a–6d**

Compounds	$\Delta\lambda_{max}$[a] (nm)	% Hypochromism[b]	K_b (M^{-1})
4a	8	7.7	1.9×10^3
4b	2	6.2	1.4×10^3
4c	2	5.2	2.5×10^3
4d	2	5.6	7.6×10^4
5a	4	12.3	1.4×10^4
5b	1	13	2.1×10^4
5c	1	29	9.4×10^4
5d	3	8.1	7.8×10^5
6a	1	8	2.6×10^4
6b	3	10	3.0×10^4
6c	4	9	9.1×10^4
6d	–	11	8.1×10^5

[a] For details of wavelength shifts, please see Supplementary data.
[b] % Hypochromicity ($H\%$) = $[(A_f - A_b)/A_f] \times 100$, where A_f and A_b represent the absorbance of free and bound compounds.

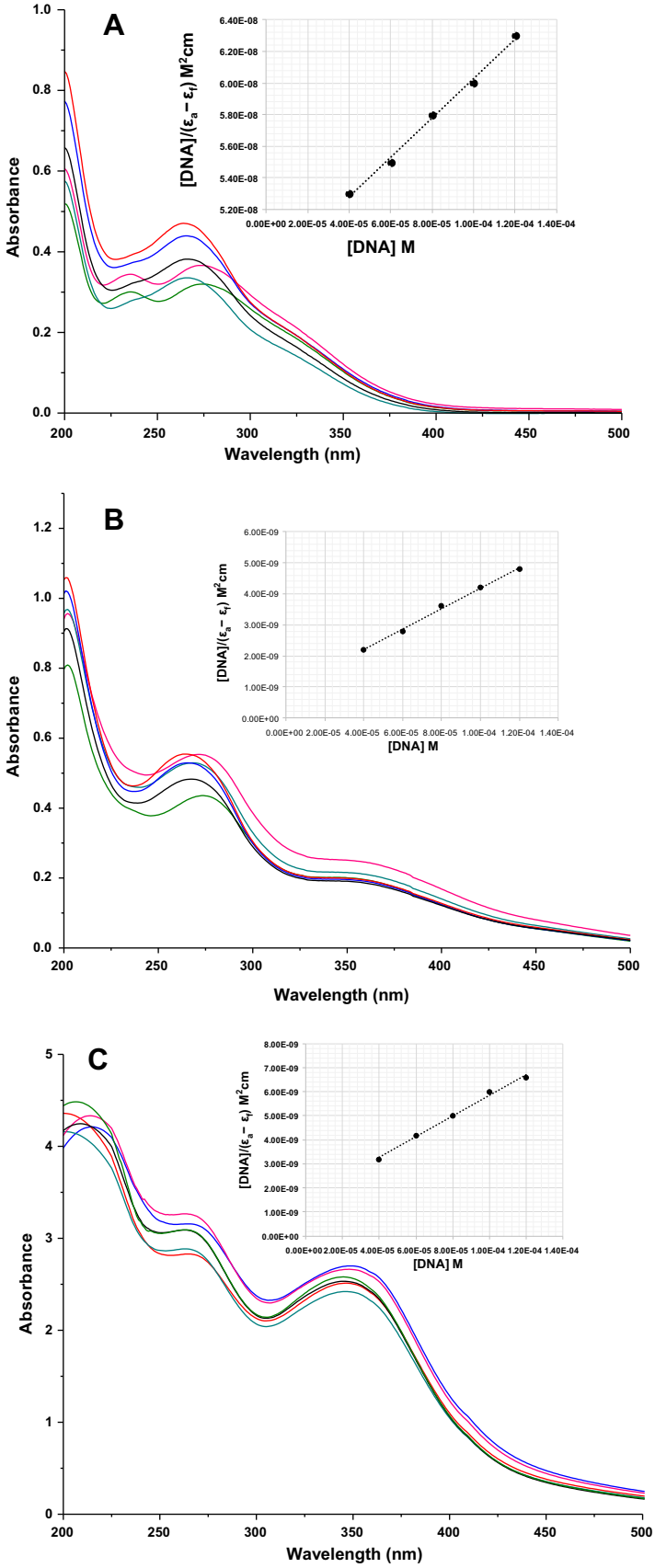

Figure 4. Absorption spectra of compound (A) DNA binding spectra of compound **4a**, (B) DNA binding spectra of compound **5a** and (C) DNA binding spectra of compound **6a** in the presence of increasing amount of Ct-DNA. Inset: plots of $[DNA]/\varepsilon_a - \varepsilon_f$ (M^2 cm^{-1}) versus [DNA] for the titration of CT DNA with compounds. Experimental data points; full lines, linear fitting of the data. [Compounds] 2.0×10^{-4} M, [DNA] 0.4–1.2×10^{-4} M.

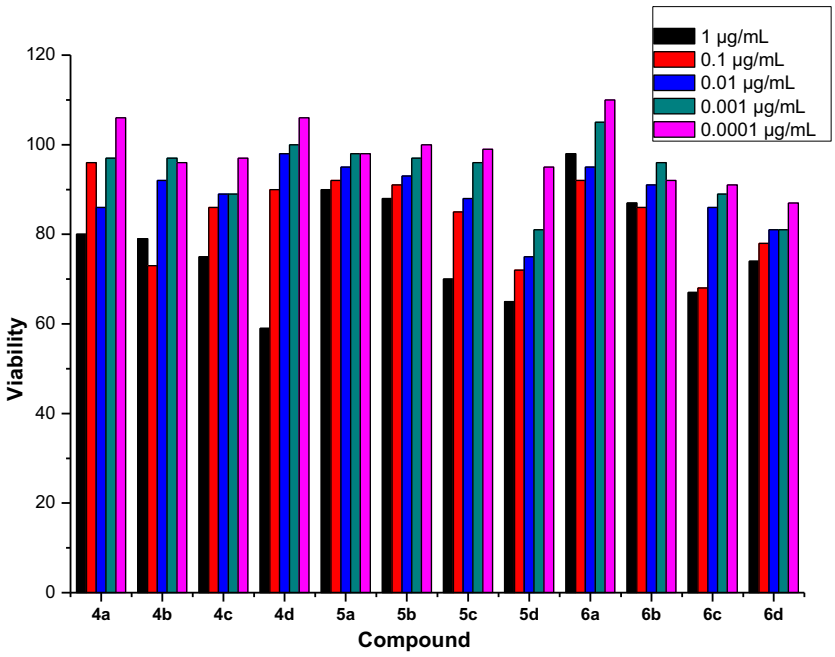

Figure 5. MCF-7 percent cell line viabilities of the synthesized compounds at 1.0, 0.1, 0.01, 0.001 & 0.0001 μg/mL concentrations.

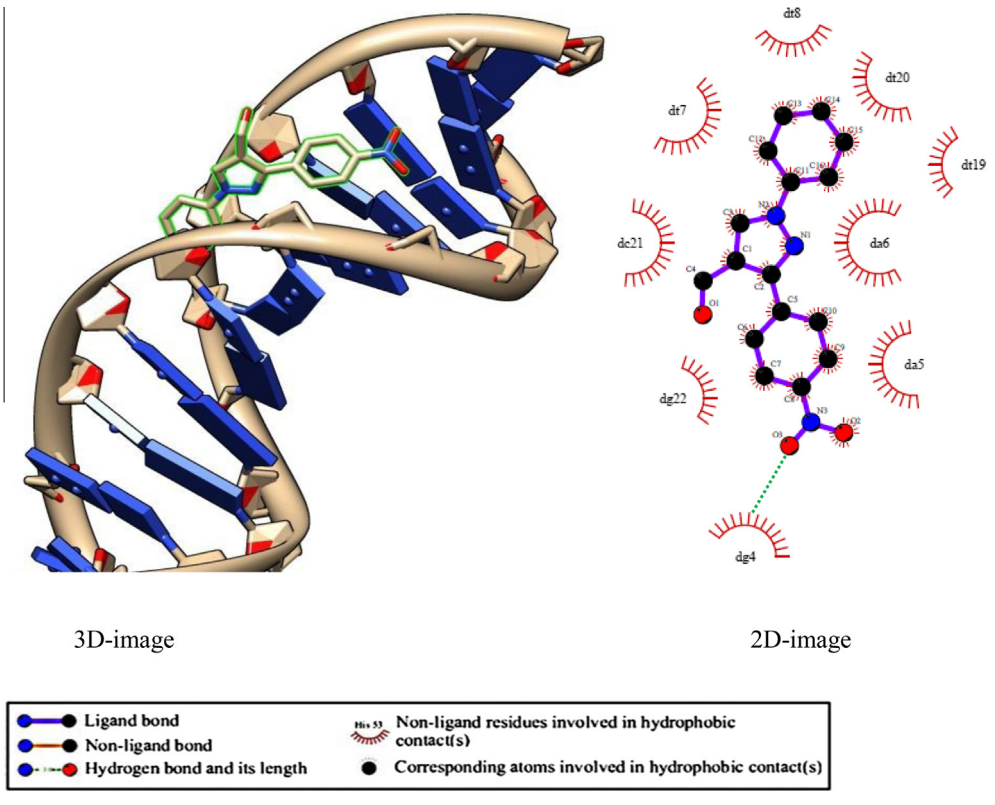

Figure 6a. 3D- and 2D-docking images of compound **4a**, depicting its vicinity with DNA.

using Microsoft Excel programme for DNA binding studies. It has been found that the standard deviation (SD) ranged from ±0.10 to ±0.11 while the correlation coefficient (R^2) and confidence levels were 0.9996–0.9999% and 98.5–99.5%, respectively. The order of DNA binding constants for these compounds was **6d > 5d > 5c > 6c > 4d > 6b > 6a > 5b > 5a > 4c > 4a > 4b**. It can be concluded from these results that the compounds **4a–6d** partially intercalated (**4a–d** through minor groove while **5a–6d** through major groove, depending upon their sizes) with Ct-DNA.[41] These results were interesting as pyrazolealdehydes (**4a–d**) favored to enter minor grooves while curcumin embedded pyrazole (**5a–d**) and their Schiff's bases (**6a–d**) preferred major grooves. Literature data indicated that the compound, forming complex with DNA minor groove, is stabilized mainly by hydrogen bonds and hydro-

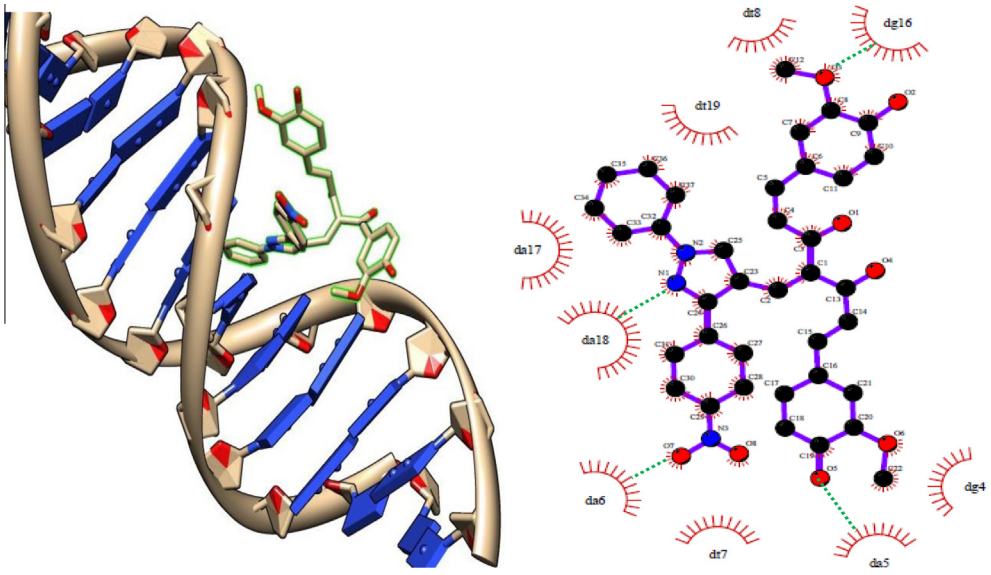

Figure 6b. 3D- and 2D-docking images of compound **5a**, depicting its vicinity with DNA.

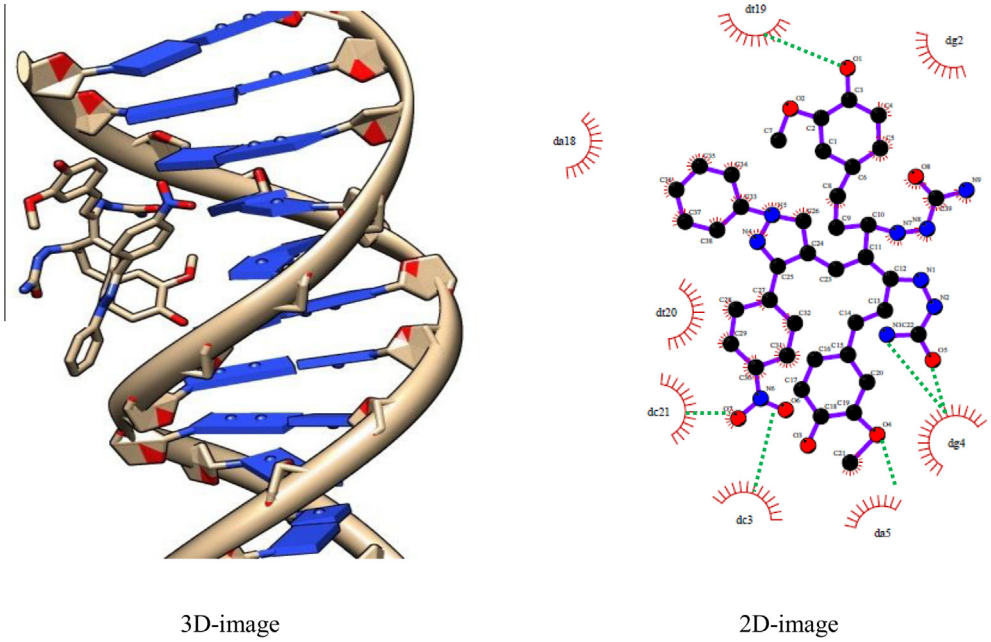

Figure 6c. 3D- and 2D-docking images of compound **6a**, depicting its vicinity with DNA.

phobic interactions.[42,43] This fact is well established by DNA titration experiments and docking studies and can be seen in Figure 6a–c and Figure FS2–S4 (Supplementary data). It is interesting to note that the compounds containing halogen group (chloro) (**4d**, **5d** and **6d**) had high affinity for DNA (higher K_b values). On the other hand, compounds containing nitro group had better DNA affinity than compounds having hydroxyl group. These results are in the agreement of the earlier reported work.[32]

2.3.3. Cell line profiles

The potential anticancer efficacy of the developed derivatives was ascertained in term of % viability on human breast cancer cell line (MCF-7, wild-type). The % viabilities of the synthesized compounds (**4a–6d**); at varying concentrations (0.0001, 0.001, 0.01, 0.1 and 1.0 μg/mL) were determined (Fig. 5).

From the figure, it can be concluded that the pyrazolealdehydes derivatives (**4a–d**) had viability of 80%, 79%, 75% and 59% at 1.0 μg/mL, respectively. On the other hand, compound **5a–d** showed 90%, 88%, 70% and 65% viability at the same concentration. Schiff's bases of the Knoevenagel's condensates (**6a–d**) showed viabilities of 98%, 87%, 74% and 67%, respectively. Thus, compounds **4d**, **5d** and **6d** had poor viability (**4d** > **5d** > **6d**) indicating good anti-cancer potential. The increase in viability of the cell line might be attributed to the increased molecular weights and hydrophobicities of the reported compounds. Recently, Bayomi et al.[44] assessed % viability of some derivatives of curcumin-I on human breast cancer cell line

(MCF-7; MDR). It was observed that cell line viabilities of these compounds were 19–94% at 20 μg/mL. It is interesting to note that this concentration was higher than the reported ones in this article (59% viability at 1.0 μg/mL; low concentrations).

2.4. Molecular simulation

2.4.1. DNA docking

The combinatorial chemistry and virtual screening have achieved good reputation in drug discovery by reducing extremely time-consuming steps of synthesis and biological screening. Besides, docking approach is a good tool for predicting the interactions of drugs at bio-molecular level. Most biologically prevalent type of DNA is B-form, which has characteristic wide and deep major grooves and narrow and deep minor grooves. Base pairing between two DNA strands gives rise to the distinct hydrogen bond acceptor/donor patterns in the major and minor grooves. The rigid molecular DNA docking of the compounds had been carried out using AutoDock 4.0 tool to find out the possible sites of DNA interactions with the reported compounds. The docking studies of the compounds were performed with DNA dodecamers $d(CGCGAATTCGCG)_2$ (PDB ID: 1BNA). The docking energies of the synthesized compounds followed the order: **6d > 6a > 6b > 6c > 5d > 5b > 5c > 5a > 4d > 4b > 4a > 4c**. The docked models of first members of all the three series (**4a**, **5a** and **6a**) are shown in Figure 6a–c. It is clear from these figures that low molecular weight compounds (**4a**) preferred DNA minor grooves. Besides, it is interesting to note that the binding sites shifted from minor to major grooves as the size of the molecules increased. Therefore, compounds **5a and 6a** interacted through the major grooves of DNA.

The numbers of H- bonds formed by the compounds **4a**–**6d** are given in Table 2. Other bondings such as Van der Waal's forces, electrostatic and hydrophobic interactions are given in Table TS2 (Supplementary data). The number of hydrogen bonds were one (**4a** and **4c**), two (**4b** and **4d**), four (**5a**–**d**), six (**6a**), four (**6b** and **5d**) and three (**6c**). During the process of DNA interaction, compounds **4a**–**d** oriented themselves in such a fashion that their *N*-phenyl rings and formyl groups were inside DNA minor groove while other phenyl rings; carrying functional groups; were outside the groove. This molecular arrangements led to the formation of two H-bonds (**A**: DT8:O3′::O of hydroxyl group & **B**: DA18:H3::O of carbonyl group) in **4b** and one in **4c** (**A**: DG4:H22::O of carbonyl group). In compound **4a**, the ring carrying functional group got twisted and formed one H bond (**A**: DG4:H22::O of nitro group) with guanine moiety. This twisting of the ring might be due to two reasons (i) GC rich region has large positive potential responsible for molecular attraction[45] and (ii) more repulsion from backbone phosphate groups; compelling the ring to twist from normal planar geometry. On the insertion of curcumin (**5a**–**d**), the only effect was increase in the molecular size shifting DNA interaction from minor to major grooves. In these compounds, total four hydrogen bonds were formed with common bonds between carbonyl and methoxy groups of the curcumin. The order of docking energy among these compounds was: **5d > 5b > 5c> 5a**; similar to the compounds of previous series (chloro derivative more interacting than the compounds of respective series). Furthermore, in Schiff's bases of Knoevenagel's condensates (**6a**–**d**), the order of docking energy was **6d > 6a > 6b > 6c**. The replacement of carbonyl groups by disemicarbazone moiety increased the tendency of the molecules to form more hydrogen bonds. Therefore, the numbers of hydrogen bonds were six, four, three and four in **6a**, **6b**, **6c** and **6d**, respectively. Greater numbers of hydrogen bonds were observed in the case of **6a** due to the presence two oxygen (Nitro group). The carbonyl and amino moieties were the common groups involved in H-bonding in this series. Briefly, the experimental results of DNA binding are well supported by the results of docking studies. Compound bearing 3-nitro substituent in phenyl ring had less affinity (high binding energy −7.44 kcal/mol), while compounds having 4-nitro and 2-hydroxy had more affinity (low binding energy −7.74 and −7.96 kcal/mol, respectively). These phenomena can be explained by considering the non-covalent interactions such as hydrogen bonds, Van der Waal's forces, electrostatic and hydrophobic bonds. The docking energy ($\Delta G_{binding}$) produced by AutoDock is sum of various factors as:

$$\Delta G_{binding} = \Delta G_{vdW} + \Delta G_{elec} + \Delta G_{hbond} + \Delta G_{desolv} + \Delta G_{tors}$$

Interestingly, it can be seen that, the sum of Vdw + Hb + dissolvation energy is quite high (Table TS2, Supplementary data) in the case of 3-nitro substituent's (**4c**, **5c** and **6c**). Van der Wall's contacts of the first compounds of each series are shown in Figures FS2–FS4 (Supplementary data). It is clear from the figures binding site is shifted from minor to major grooves on increasing size of molecule. Furthermore, it may be observed from these figures that Van der Wall's contacts decreased on increasing molecular size. In the present study the docking energies and in vitro cell line viabilities were estimated. Regression analyses results were found to be satisfactory with ±0.08, ±0.10, 0.9997–0.9999% and 99.0–99.5% values of standard deviation, correlation coefficient (R^2) and confidence levels, respectively. Basically, the presence of 3-nitro group into the ring destabilizes DNA–ligand adduct by varying these terms (Table TS2, Supplementary data). Hence, it is clearly indication that electrostatic interactions (including H-bonding) and Van der Wall's interactions were the major factor which determines the site of DNA binding with the compounds. All these results are in agreement with the observations obtained from experimental results. Based on these facts, it may be concluded that the docking results are comparable with the DNA binding studies.

2.4.2. Mechanism of action at supramolecular level

UV–vis spectroscopic data indicated that the reported compounds formed adducts with DNA due to covalent and non-covalent bindings. The docking studies had also shown that compounds **4a**–**d** interacted with the nucleic acid in the minor grooves of DNA. On the other hand, larger sizes of the compounds **5a**–**6d** compelled them to interact with in major groves. These results tallied well with the finding of Hamilton et al.[46] Therefore, compounds of series **4a**–**d** were attracted towards minor groves while compounds of series **5a**–**d** and **6a**–**d** for major grooves. A deep insight of interactions at supramolecular level was visualized and developed by docking studies. For this purposes 3-D docking models were developed for all the compounds and only three are shown in Figure 6a–c (first compounds of each series). The critical evaluation and 3D visualization of compound **4a** model (Figure 6a) indicated that 4-nitro-phenyl moiety is inside the minor groove while the remaining part is outside. Nitro group was forming one hydrogen bond with guanine-cytosine base pair (Table 2). The hydrogen bonding involved the participation of oxygen atom of nitro group and hydrogen atom of guanine. Similarly, in case of compound **5a** (Figure 6b), 4-nitro-phenyl moiety was inside the major groove while the remaining part stay outside the groove. Total four hydrogen bonds were formed in this process (three inside and one outside of groove). Inside hydrogen bonds were formed between (i) oxygen atom of nitro group and hydrogen atom of adenine, (ii) oxygen atom of methoxy group and hydrogen atom of guanine and (iii) nitrogen atom of pyrazole ring and hydrogen atom of adenine. On the other hand, outside hydrogen bonds were formed between hydrogen atom of hydroxyl group and oxygen of phosphate group (Table 2). In case of compound **6a** (Figure 6c), five hydrogen bonds were formed inside major groove while one outside grooves. The inside hydrogen bonds were formed between (i) hydrogen of hydroxyl group at curcumin part and oxygen of thymine,

Table 2
DNA docking data of compounds **4a–6d**

Compounds	No. of H-bond with DNA	Residues involved in H-bonding bonding (*Bond length*)
4a	1	**A**: DG4:H22::O of nitro (*1.69*)
4b	2	**A**: DT8:O3′::O of hydroxyl group (*2.70*) **B**: DA18:H3::O of carbonyl group (*2.07*)
4c	1	**A**: DG4:H22::O of carbonyl group (*2.31*)
4d	–	–
5a	4	**A**: DA5:$OP_{2:}$:O of hydroxyl group (*2.83*) **A**: DA6:H7::O of nitro group (*2.07.*) **B**: DG16:H7::UNK0:O of methoxy group (*1.78*) **B**: DA18:H7::UNK0:N of pyrazole ring (*1.89*)
5b	4	**B**: DA18:H7::UNK0:O of carbonyl group (*2.09*) **A**: DA5:H7::UNK0:O of hydroxyl of pyrazolealdehydes (*1.73*) **A**: DA6:H7::UNK0:O of methoxy group (*2.08*) **A**: DG4:H7::UNK0:N of pyrazole ring (*2.19*)
5c	4	**A**: DA5:H62::UNK0:O of Nitro group (*2.09*) **B**: DG16:H7::UNK0:O of methoxy group (*2.33*) **A**: DA5:H7::UNK0:O of nitro group (*1.83*) **B**: DA17:H7::UNK0:O of carbonyl group (*1.70*)
5d	–	–
6a	6	**B**: DT19:O4 H UNK0::O of hydroxyl of curcumin (*3.10*) **A**: DA5:H62::UNK0:O of methoxy group (*2.42*) **A**: DG4:OP2:UNK0:N of amino group (*2.70*) **A**: DG4:H7::UNK0:O of carbonyl of amide group (*1.89*) **B**: DC21:H41::UNK0:O of nitro group (*2.04*) **A**: DC3:H4::UNK0:O of nitro group (*2.14*)
6b	4	**B**: DT19:OP2 H::UNK0:O of hydroxyl of curcumin (2.58) **A**: DG4:H7::UNK0:O of carbonyl of amide group (2.02) **A**: DG2:OP_2::UNK0:O of hydroxyl groupof pyrazolealdehyde (*3.0*) **B**: DG22:H7 -:UNK0:O of methoxy group (*2.19*)
6c	3	**B**: DG16:OP_1::UNK0:N of amide group (*2.89*) **B**: DA18:H7::UNK0:O of nitro group (*2.20*) **B**: DA18:OP_2::UNK0:O hydroxyl of curcumin (*2.72*)
6d	–	–

Where '**A**' & '**B**' refers to the chains of DNA while 'UNKO' refers to the respective ligands.

(ii) oxygen of methoxy group at curcumin part and hydrogen of adenine, (iii) oxygen of amide and hydrogen of guanine, (iv) oxygen of nitro group and hydrogen of cytosine and (v) oxygen of nitro group and hydrogen of cytosine. Outside hydrogen bond was formed between hydrogen of amino group of compound and oxygen of phosphate group of DNA. Therefore, it might be concluded that hydrogen bonding was the major force for the interactions of the reported compounds with DNA. Besides, other forces such as Van der Waal's, steric effect, etc. are contributing in binding of ligands to the DNA. Based on the above discussion, it can be concluded that the compounds of series **6a–d** had stronger affinity towards DNA than the compounds of series**4a–d** and **5a–d**, which was in accordance with the experimental UV–vis spectroscopic data.

3. Future perspectives of the reported compounds

The future perspectives of the reported compounds can be assessed and predicted by considering their various properties such as hemolysis, cell line viabilities, DNA binding constants and

Table 3
The comparative properties of the synthesized compounds (**4a–6d**)

Compd	% Hemolysis	% Viabilities (μg/mL)					DNA Binding const. (K_b, M^{-1})	% Hypochromism	Docking energy (kcal/mol)
		1	0.1	0.01	0.001	0.0001			
4a	7	80	96	86	97	106	1.9×10^3	7.7	−8.26
4b	18	79	73	92	97	96	1.4×10^3	6.2	−8.45
4c	10	75	86	89	89	89	2.5×10^3	5.2	−7.39
4d	9	59	90	98	98	100	7.6×10^4	5.6	–
5a	10	90	92	95	98	98	1.4×10^4	12.3	−10.59
5b	20	88	91	93	97	100	2.1×10^4	13	−11.72
5c	14	70	85	88	96	99	9.4×10^4	29	−10.88
5d	16	65	72	75	81	95	7.8×10^5	8.1	–
6a	11	98	92	95	105	110	2.6×10^4	8	−13.48
6b	25	87	86	91	91	92	3×10^4	10	−12.64
6c	16	67	68	86	89	91	9.1×10^4	9	−12.48
6d	17	74	78	81	81	87	8.1×10^5	11	–

docking energies. For this purpose, these properties are summarized in Table 3. It is clear from this table that hemolysis values ranged from 7% to 25%, which is much lower than the standard doxorubicin drug (~42% at 100 μg/mL). Therefore, the reported compounds are less toxic to normal cells in comparison to the standard drug. The anticancer profiles in terms of % viabilities ranged from 59% to 79% at 1.0 μg/mL; indicating quite good potential of their anticancer candidatures. The values of DNA binding constant ranged from 1.4×10^3 to 8.1×10^5 M^{-1}, indicating the compounds as potential anticancer agents. These results have also been supported by the docking data. It is interesting to note that DNA binding constants were in the order: series **6a–d >** series **5a–d >** series **4a–d**, but the order of the anticancer activities was just reverse. The possible reason for above said behavior of these compounds is the direct binding with DNA without any hurdle (biological membranes and other enzymes). On the other hand, in case of cell line viabilities, these compounds had to pass the cell and nuclear membrane barriers via passive transport mechanism. Probably, the compounds of series **6a–d** and **5a–d** were less allowed to pass through these membranes due to their bigger size, while the compounds of series **4a–d** might be able to pass these barriers efficiently due to small size. Based on these discussions, the future of the developed compounds seems to be quite bright as anticancer agents.

4. Experimental section

4.1. Materials and methods

4.1.1. Chemicals and reagents

The rhizome of *C. longa* was collected from the agricultural field, New Delhi, India. The plant was identified by observing its taxonomical features. Phenyl hydrazine, *ortho*-hydroxyacetophenone, *para*-nitroacetophenone, *meta*-nitroacetophenone, *para*-chloroacetophenone, phosphorus oxychloride and dimethylformamide were obtained from Spectrochem Ltd, Mumbai, India. Semicarbazide hydrochloride and *tris*-(hydroxymethyl)aminomethane were obtained from Sisco Research Lab., Mumbai, India and S.D. Fine Chem. Ltd, New Delhi, India. Ethanol, methanol, chloroform, dichloromethane and hexane of HPLC grades were purchased from Merck, Mumbai, India. Ct-DNA (as sodium salt) was obtained from SRL Pvt. Ltd, Mumbai, India. The concentrations of DNA were determined spectrometrically with an extinction coefficient of 6600 M^{-1} cm^{-1} at 258 nm. Silica gel G (10–40 μm) for thin layer chromatography (TLC) and normal silica gel (60–120 μm) for column chromatography were supplied by Merck, Mumbai, India. Tris–HCl buffer (2.0×10^{-2} M) was prepared in Millipore water at pH range of 7.2–7.3.

4.2. Instruments used

Elemental analyses were determined by using Vario EL elemental analyzer. UV–vis spectra were obtained by T80 UV–vis spectrophotometer. FT-IR spectra were obtained in the range of 4000–400 cm^{-1} on a Nicolet FT-IR spectrometer. ^1H nuclear magnetic resonance (^1H NMR) spectra were recorded using Bruker 300 MHz instrument. ESI-MS were performed by micrOTOF-Q II Electrospray ionization mass spectrometer (Bruker). Ultraviolet (UV) cabinet was used to view thin layer chromatograms. pH meter of control dynamics was used to record pH of the solutions. Melting points were determined on Veego instrument and were uncorrected. HPLC system of ECOM (Czech Republic) consisting of solvent delivery pump (Alpha 10), manual injector, absorbance detector (Sapphire 600 UV–Vis), chromatography I/F module data integrator (Indtech. Instrument, India) and Winchrome software was used to determine the purity of compounds. The column used was Sunniest C_{18} (150 × 4.5 mm, 5.0 μm) Chromanik, Japan.

4.3. Separation of curcumin

Curcumin-I was separated by earlier reported method.[47] Briefly, a mixture of curcumin was loaded onto a silica gel column impregnated with $NaHCO_3$ and eluted with pure dichloromethane. The purity of the eluted component was checked by HPLC.

4.4. Procedure of the preparation of phenyl hydrazones

1:1 Mixture of phenylhydrazine (**1**) and substituted acetophenone (**2a–d**) was refluxed in ethanol for 8–12 h. The progress of the reaction was monitored by TLC. After the completion of the reaction, the solid product was filtered and washed with cold ethanol.

4.4.1. Procedure of the preparation of 3-substituted-1-phenyl-1*H*-pyrazole-4 carbaldehydes

Vilsmeier–Haack reaction: $POCl_3$ (50 mM) was added drop wise to anhydrous DMF (50 mM) in round bottom flask (250 mL) at 0 °C. The reaction mixture was stirred for 30–45 min until the formation of Vilsmeier's complex appeared. The corresponding phenylhydrazone (**3a–d**, 25 mM) was dissolved in minimum amount of DMF and added to Vilsmeier's complex (50 mM). The reaction mixture was stirred for 30 min at room temperature and then refluxed for 15–16 h. The reaction mixture was poured into water/ice and kept for 5–10 min. The reaction mixture was neutralized by 2.0 N NaOH with stirring for 30 min. The precipitated product was filtered and the solid obtained crystallized using chloroform.

4.4.1.1. 3-(4-Nitrophenyl)-1-phenyl-4,5-dihydro-1*H*-pyrazole-4-carbaldehyde (4a). Yield: 80%, mp 158–160–162 °C; Anal. Calcd: C (65.53%), H (3.78%), N (14.33%), O (16.37%), found: (65.56%), H (3.80%), N (14.35%), O (16.36%) IR ν_{max} (cm^{-1}): 3110 (Ar-H), 1686 (CHO), 1627 (C=N), 1584 (C=C), N–O (1345). ^1H NMR ($CDCl_3$) δ (ppm): 10.10 (s, 1H, CHO), 8.60 (s, 1H, pyrazole-H), 8.38 (d, 2H, J = 8.7 Hz, Ar-H), 8.20 (d, 2H, J = 6.9 Hz, Ar-H), 7.84 (t, 3H, J = 8.1 Hz Ar-H), 6.69–7.62 (m, 2H, Ar-H). ESI-MS (m/z) Calcd for $C_{16}H_{11}N_3O_3$: 293.27, found: 293.94.

4.4.1.2. 3-(2-Hydroxyphenyl)-1-phenyl-4,5-dihydro-1*H*-pyrazole-4-carbaldehyde (4b). Yield: 75%, mp 208–210 °C; Anal. Calcd: C (72.72%), H (4.58%), N (10.6%), O (12.11%), found: C (72.71%), H (4.58%), N (10.5%), O (12.10%). IR ν_{max} (cm^{-1}): 3550 (OH), 3125 (Ar-H), 1680 (CHO), 1625 (C=N), 1590 (C=C). ^1H NMR ($CDCl_3$) δ (ppm): 9.938 (s, 1H, CHO), 8.92 (s, 1H, OH), 8.52 (s, 1H, pyrazole-H), 7.80–7.73 (m, 4H, Ar-H), 7.60 (t, 2H, J = 7.2 Hz, Ar-H), 7.39 (t, 1H, J = 6.9 Hz, Ar-H), 6.98 (d, 2H, J = 8.4 Hz, Ar-H). ESI-MS (m/z) Calcd for $C_{16}H_{12}N_2O_2$ [M+Na]: 287.26, found: 287.17.

4.4.1.3. 3-(3-Nitrophenyl)-1-phenyl-4,5-dihydro-1*H*-pyrazole-4-carbaldehyde (4c). Yield: 68%, mp 141–142 °C; Anal. Calcd: C (65.53%), H (3.78%), N (14.33%), O (16.37%), found: C (65.54%), H (3.79%), N (14.36%), O (16.38%). IR ν_{max} (cm^{-1}): 3120 (Ar-H), 1688 (CHO), 1583 (C=C), 1620 (C=N), 1347 (N–O). ^1H NMR ($CDCl_3$–300 MHz) δ (ppm): 10.09 (s, 1H, CHO), 8.58 (s, 1H, pyrazole-H), 8.35–8.29 (m, 2H, Ar-H), 7.83 (t, 2H, J = 7.2 Hz, Ar-H), 7.70–7.65 (m, 1H, Ar-H), 7.58–7.52 (m, 3H, Ar-H), 7.49–7.41 (m, 1H, Ar-H). ESI-MS (m/z) Calcd for $C_{16}H_{11}N_3O_3$ $[M+Na]^+$: 316.26, found: 316.20.

4.4.1.4. 3-(4-Chlorophenyl)-1-phenyl-4,5-dihydro-1*H*-pyrazole-4-carbaldehyde (4d). Yield: 85%, mp 147–148 °C; Anal. Calcd: C (67.97%), H (3.92%), Cl (12.54%), N (9.91%), O (5.66%), found: C (68.10%), H (3.98%), Cl (12.55%), N (9.92%), O (5.67%). IR ν_{max} (cm^{-1}): 3115 (Ar-H), 1690 (CHO), 1625 (C=N), 1579 (C=C). ^1H NMR ($CDCl_3$) δ (ppm): 9.97 (s, 1H, CHO), 7.64 (d, 2H, J = 7.2 Hz, Ar-H), 7.48 (t, 2H, J = 6.6 Hz, Ar-H), 6.91 (d, 2H, J = 7.5 Hz, Ar-H), 6.31–6.12(m, 3H, Ar-H), 9.21 (s, 1H, pyrazole-H). ESI-MS (m/z) Calcd for $C_{16}H_{11}ClN_2O$: 282.72, found: 283.15.

4.4.2. Procedure for the synthesis Knoevenagel condensates of curcumin-I

3-(Substituted)-1-phenyl-1*H*-pyrazole-4-carbaldehyde (1.0 mM in 25 mL chloroform) was added into a solution of curcumin (1.0 mM in 25 mL chloroform) in round bottom flask (100 mL). Piperidine (2–5%) was added in the mixture and stirred at room temperature for 48–55 h. After the completion of the reaction, chloroform was reduced and the solid product was washed with DCM/MeOH (99:1, v/v) to remove impurities.

4.4.2.1. 1,7-Bis(4-hydroxy-3-methoxyphenyl)-4-{[3-(4-nitrophenyl)-1-phenyl-1*H*-pyrazol-4-yl]methylidene}hepta-1,6-diene-3,5-dione (5a). Yield: 65%, 141–142, mp 91 °C; Anal. Calcd: C (69.04%), H (4.54%), N (6.53%), O (19.89%), found: C (69.06%), H (4.58%), N (6.52%), O (19.90%). IR ν_{max} (cm^{-1}): 3506 (OH), 1687 (C=O), 1454 (C=C), 1338 (NO_2), 1026 (Ar-O–C). ^1H NMR ($CDCl_3$) δ (ppm): 8.18 (d, 2H, J = 7.5 Hz, Ar-H), 8.11 (s, 2H, Ar-H), 8.03 (d, 2H, J = 6.6 Hz, Ar-H), 7.77 (s, 1H, =CH-Ar), 7.66–7.56 (m, 2H, Ar-H), 7.36 (d, 2H, J = 6.9 Hz, Ar-H), 6.62 (d, 3H, J = 8.1 Hz, Ar-H), 6.62–6.59 (m, 3H, Ar-H), 6.56 (d, 2H, J = 13.2 Hz, HC=C–), 7.83 (d, 2H, J = 15.6 Hz, HC=C–C=O), 8.59 (s, pyrazole-H), 3.98 (s, 6H, OCH_3). ESI-MS (m/z) Calcd for $C_{37}H_{29}N_3O_8$: 643.64, found: 642.30.

4.4.2.2. 1,7-Bis(4-hydroxy-3-methoxyphenyl)-4-{[3-(2-hydroxyphenyl)-1-phenyl-1*H*-pyrazol-4-yl]methylid ene}hepta-1,6-diene-3,5-dione (5b). Yield: 69%, mp 101–102 °C; Anal. Calcd: C (72.3%), H (4.92%), N (4.56%), O (18.22%), found: C (72.1%), H (4.93%), N (4.55%), O (18.26%); IR ν_{max} (cm^{-1}): 3510 (OH), 1685 (C=O), 1490 (C=C), 1024 (Ar-O–C). ^1H NMR ($CDCl_3$) δ (ppm): 8.52 (s, pyrazole-H), 8.21 (d, 2H, J = 7.2 Hz, Ar-H) 8.04 (s, 2H, Ar-H), 7.83 (d, 2H, J = 15.2 Hz, HC=C–C=O), 7.82–7.73 (m, 4H, Ar-H), 7.76 (s, 1H, =CH-Ar), 7.61 (d, 2H, J = 8.1 Hz Ar-H), 7.41 (t, 2H, J = 6.9 Hz, Ar-H), 6.65–6.63 (m, 3H, Ar-H), 6.51 (d, 2H, J = 12.6 Hz, HC=C–),3.80 (s, 6H, OCH_3). ESI-MS (m/z) Calcd for $C_{37}H_{30}N_2O_7$: 635.61 $[M+Na-2H]^+$, found: 633.12.

4.4.2.3. 1,7-Bis(4-hydroxy-3-methoxyphenyl)-4-{[3-(3-nitrophenyl)-1-phenyl-1*H*-pyrazol-4-yl]methylidene}-hepta-1,6-diene-3,5-dione (5c). Yield: 63%, mp 110–112 °C; Anal. Calcd: C (69.04%), H (4.54%), N (6.53%), O (19.89%), Found: (69.2%), H (4.72%), N (6.55%), O (19.91%), IR ν_{max} (cm^{-1}): 3468 (OH), 1689 (C=O), 1472 (C=C), 1347 (NO), 1025 (Ar-O–C), ^1H NMR ($CDCl_3$) δ (ppm): 8.58 (s, pyrazole-H), 8.37–8.27 (m, 2H, Ar-H), 8.16 (d, 2H, J = 12.3 Hz, HC=C–C=O), 7.92 (s, 1H, Ar-H), 7.76 (s, 1H, =CH-Ar), 7.39 (d, 2H, J = 12 Hz, HC=C–), 7.69 (t, 3H, J = 8.1 Hz, Ar-H), 7.44 (d, 3H, J = 7.2 Hz, Ar-H), 6.64 (t, 1H, J = 6.0 Hz, Ar-H), 6.63–6.52 (m, 3H, Ar-H), 3.99 (s, 6H, OCH_3). ESI-MS (m/z) Calcd for $C_{37}H_{29}N_3O_8$: 666.63 $[M+Na]^+$, found: 666.88.

4.4.2.4. 1,7-Bis(4-hydroxy-3-methoxyphenyl)-4-{[3-(4-chlorophenyl)-1-phenyl-1*H*-pyrazol-4-yl]methylidene}-hepta-1,6-diene-3,5-dione (5d). Yield: 60%, mp; 115–117 °C; Anal. Calcd: C (70.19%), H (4.62%), Cl (5.6%), N (4.42%), O (15.16%), Found: C (70.22%), H (4.68%), Cl (5.7%), N (4.44%), O (15.18%) IR ν_{max} (cm^{-1}): 3507 (OH), 1718 (C=O), 1424 (C=C), 1330 (NO_2), 1033 (Ar-O–C). ^1H NMR ($CDCl_3$) δ (ppm):8.62 (s, pyrazole-H), 8.31 (d, 2H, J = 8.1 Hz, Ar-H,) 8.10 (s, 2H, Ar-H), 7.87–7.86 (m, 3H, Ar-H), 7.82 (d, 2H, J = 15.3 Hz, HC=C–C=O), 7.82 (s, 1H, =CH-Ar), 7.60 (d, 2H, J = 7.5 Hz Ar-H), 6.67 (t, 2H, J = 7.2 Hz, Ar-H), 6.56–6.54 (m, 4H, Ar-H), 6.43 (d, 2H, J = 12.3 Hz, HC=C–), 3.70 (s, 6H, OCH_3). ESI-MS (m/z) Calcd for $C_{37}H_{29}ClN_2O_6$: 633.08, found: 633.21.

4.4.3. Procedure for the synthesis of Schiff base of Knoevenagel Condensates

Each curcumin-I condensate (**5a**–**d**); (1.0 mM) was dissolved in minimum amount of chloroform. Semicarbazide hydrochloride (2.0 mM; in 20 mL methanol with a drop of water to dissolve the salt) was added to the curcumin condensate solution drop wise. A small amount of catalyst (piperidine) was also added to the above reaction mixture. The reaction mixture was stirred for 24 h. After the completion of the reaction, the product was concentrated and washed repeatedly.

4.4.3.1. 5-[(Carbamoylamino)imino]-1,7-bis(4-hydroxy-3-methoxyphenyl)-4-{1-[3-(4-nitroyphenyl)-1-phenyl-4,5-dihydro-1*H*-pyrazol-4-ylidene]ethyl}hepta-1,6-dien-3-ylidene]amino]urea (6a). Yield: 60%, mp 125–126 °C; Anal. Calcd: C (61.82%), H (4.66%), N (16.64%), O (16.89%), Found: C (61.62%), H (4.56%), N (16.54%), O (16.29%), IR ν_{max} (cm^{-1}): 3580 (NH), 3512 (OH), 1699 (C=O), 1598 (C=N), 1337 (Ar-N–O), 1450 (C=C), 1338 (NO_2), 1020 (Ar-O–C). ^1H NMR ($CDCl_3$) δ (ppm): 8.57 (s, pyrazole-H), 8.17 (d, 2H, J = 7.5 Hz, Ar-H), 8.10 (s, 2H, Ar-H), 8.13 (d, 2H, J = 7.2 Hz, Ar-H), 7.83 (d, 2H, J = 15.6 Hz, HC=C–C=O), 7.78 (s, 1H, =CH-Ar), 7.65–7.62 (m, 2H, Ar-H), 7.40 (d, 2H, J = 6.9 Hz, Ar-H), 6.61 (d, 3H, J = 8.1 Hz, Ar-H), 6.54–6.52 (m, 3H, Ar-H), 6.36 (d, 2H, J = 13.2 Hz, HC=C–), 3.98 (s, 6H, OCH_3) 2.68 (bs, 4H, NH_2). ESI-MS (m/z) Calcd for $C_{39}H_{35}N_9O_8$ $[M-OCH_3]^+$: 727.72, found: 727.39.

4.4.3.2. 5-[(Carbamoylamino)imino]-1,7-bis(4-hydroxy-3-methoxyphenyl)-4-{1-[3-(2-hydroxyphenyl)-1-phenyl-4,5-dihydro-1*H*-pyrazol-4-ylidene]ethyl}hepta-1,6-dien-3-ylidene]amino]urea (6b). Yield: 65%, mp; 130–131 °C; Anal. Calcd: C (64.28%), H (4.98%), N (15.38%), O (15.37%), Found: C (64.22%), H (4.80%), N (15.30%), O (15.39%). IR ν_{max} (cm^{-1}): 3515 (OH), 1690(C=O), 1490 (C=C), 1596 (C=N) 1022 (Ar-O–C), ^1H NMR ($CDCl_3$) δ (ppm): 8.53 (s, pyrazole-H), 8.21 (d, 2H, J = 7.5 Hz, Ar-H,) 8.14 (s, 2H, Ar-H), 7.83 (d, 2H, J = 15.0 Hz, HC=C–C=O), 7.82–7.71 (m, 4H, Ar-H), 7.76 (s, 1H, =CH-Ar), 7.60 (d, 2H, J = 7.21 Hz Ar-H), 7.41 (t, 2H, J = 8.1 Hz, Ar-H), 6.65–6.63 (m, 3H, Ar-H), 6.51 (d, 2H, J = 12.6 Hz, HC=C–), 3.80 (s, 6H, OCH_3), 2.568 (bs, 4H, NH_2). ESI-MS (m/z) Calcd for $C_{39}H_{36}N_8O_7$: 729.75 [M+1], found: 729.29.

4.4.3.3. 5-[(Carbamoylamino)imino]-1,7-bis(4-hydroxy-3-methoxyphenyl)-4-{1-[3-(3-nitrophenyl)-1-phenyl-4,5-dihydro-1*H*-pyrazol-4-ylidene]ethyl}hepta-1,6-dien-3-ylidene]amino]urea (6c). Yield: 63%, mp; 118–119 °C; Anal. Calcd: C (61.82%), H (4.66%), N (16.64%), O (16.89%), Found: C (61.78%), H (4.68%), N (16.60%), O (16.92%), IR ν_{max} (cm^{-1}): 3486 (OH), 1696 (C=O), 1585 (C=N), 1472 (C=C), 1347 (NO), 1025 (Ar-O–C). ^1H NMR ($CDCl_3$) δ (ppm): 8.57 (s, pyrazole-H), 8.26–8.14 (m, 2H, Ar-H), 8.11 (d, 2H, J = 12.3 Hz, HC=C–C=O),7.67 (s, 1H, =CH-Ar), 7.38 (d, 2H, J = 12 Hz, HC=C–), 7.68 (t, 4H, J = 7.5 Hz, Ar-H), 7.71 (d, 3H, J = 6.6 Hz, Ar-H), 6.62 (t, 2H, J = 8.1 Hz, Ar-H), 6.52–6.52 (m, 2H, Ar-H), 3.98 (s, 6H, OCH_3), 2.98 (bs, 4H, NH_2). ESI-MS (m/z) Calcd for $C_{39}H_{35}N_9O_8$ $[M-OCH_3]^+$: 727.72, found: 727.80.

4.4.3.4. 5-[(Carbamoylamino)imino]-1,7-bis(4-hydroxy-3-methoxyphenyl)-4-{1-[3-(4-chloroyphenyl)-1-phenyl-4,5-dihydro-1*H*-pyrazol-4-ylidene]ethyl}hepta-1,6-dien-3-ylidene]amino]urea (6d). Yield: 67%, mp; 120–121 °C; Anal. Calcd: C (62.69%), H (4.72%), Cl (4.74%), N (15.0%), O (12.85%), found: C (62.60%), H (4.65%), Cl (4.64%), N (14.8%), O (12.90%). IR ν_{max} (cm^{-1}): 3510 (OH), 1718 (C=O), 1580 (C=N), 1429 (C=C), 1018 (Ar-O–C), ^1H NMR ($CDCl_3$) δ (ppm): 8.62 (s, pyrazole-H), 8.31 (d, 2H, J = 8.1 Hz, Ar-H,) 8.10 (s, 2H, Ar-H), 7.87–7.86 (m, 3H, Ar-H), 7.82 (s, 1H, =CH-Ar), 7.82 (d, 2H, J = 15.3 Hz, HC=C–C=O), 7.60 (d, 2H, J = 7.5 Hz Ar-H), 6.67 (t, 2H, J = 7.2 Hz, Ar-H), 6.56–6.54 (m, 2H, Ar-H), 6.43 (d, 2H, J = 12.3 Hz, HC=C–), 3.70 (s, 6H, OCH_3), 2.72 (bs, 4H, NH_2). ESI-MS (m/z) Calcd for $C_{39}H_{36}N_8O_7$: 747.79 [M+NH_4+H], found: 748.56.

4.5. Pharmacological activities

4.5.1. Hemolysis profiles

The experimental procedure employed for the hemolytic assays of the compounds is an adjustment of ASTM standard F-756-00;[48] based on colorimetric detection of Drabkin's solution. 1.5 mL test compound was incubated in 0.214 mL of dilute blood (0.1 mL rabbit whole blood mixed with 0.9 mL PBS) at 37 °C for 3 h. Harvested hemoglobin of rabbit blood was found to be less than 220 μg/mL (basal level for hemolytic test), confirming the fresh rabbit blood use in test. After incubation, the solution was centrifuged at 3800 rpm for 15.0 min. To determine the supernatant hemoglobin, 0.8 mL of Drabkin's solution was added to 0.2 mL of supernatant and the sample was allowed to stand for 15 min. The amount of cyanmethemoglobin in the supernatant was measured at 540 nm and compared with standard curve (hemoglobin concentrations ranging from 32 to 1068 mg/mL). The percent hemolysis refers to the ratio of hemoglobin concentrations in the supernatant of a blood samples not treated and treated with test compounds. Additionally, the absorption of the test compounds was determined at 540 nm in order to eliminate the effect of absorption of test compounds. Finally, saline solution and double distilled water were used as negative and positive controls, respectively.

4.5.2. DNA binding

The stock solution of disodium salt of Ct-DNA was prepared in tris–HCl buffer (pH 7.2–7.3) and stored at 4 °C temperature. Once prepared, the stock solution was used within 4 days. The concentration of the solution was determined spectrometrically. The ratio of absorbance at 260 and 280 ($\geqslant$1.8) indicated that DNA was sufficiently free of protein. The concentration of DNA was measured using its extinction coefficient at 260 nm (6600 M^{-1} cm^{-1}) after dilutions. For the titration purpose, DNA stock solution was diluted using tris–HCl buffer. The compounds were dissolved in minimum amount of methanol (2.0×10^{-4} M). UV–vis absorption spectra were recorded after each addition of different concentrations of DNA. Absorption titration was conducted by adding varying concentrations ($0.3–2.1 \times 10^{-4}$) of DNA. The intrinsic binding constant (K_b) was determined by Eq. 1, which was originally known as Benessi–Hilderbrand equation and further modified by Wolfe et al.[49]

$$[DNA]/(\varepsilon_a - \varepsilon_f) = [DNA]/(\varepsilon_a - \varepsilon_f) + 1/K_b(\varepsilon_b - \varepsilon_f) \quad (1)$$

where the apparent absorption coefficients ε_a, ε_f, and ε_b correspond to A_{obs}/[compounds], the extinction coefficient for the compounds, and the extinction coefficient for the compounds in the fully bound form, respectively. In plots of [DNA]/($\varepsilon_a - \varepsilon_f$) versus [DNA], K_b is given by the ratio of the slope to the intercept.

4.5.3. Anticancer assays

In vitro anticancer profiles of the synthesized compounds were determined against human breast cancer cell line (MCF-7) by a cell viability assay (MTT assay).[50] DMEM (low glucose), 10% fetal bovine serum and antibiotic/anti-mycotic formed the main constituents of the culture medium. MCF-7 cells were seeded in 96-well plate at a density of 2×10^3 cells/well. These were incubated at 37 °C under a humidified atmosphere containing 5% CO_2 for 24 hrs before assay. After that, the cells were further incubated in media containing various concentrations of the test compounds. After 24 h, the medium was removed and washed with PBS. About, 20 μL of MTT solution was added to each well followed by 4 h of incubation at 37 °C. Subsequently, the medium was removed followed by an addition of 200 μL DMSO. After slowly shaking (twice) for 5 s, the absorbance of each well was determined at 570 nm. The cell viability (%) was calculated as the ratio of the number of surviving cells with test compound and blank.

4.6. Simulation studies

4.6.1. DNA docking

Docking studies were performed at Intel(R) Core(TM) i3 CPU (2.3 GHz) with XP-based operating system (Windows 2007). 2D Structures of curcumin embedded pyrazole derivatives were drawn by Marvin Sketch and then converted to 3D structures and saved in pdb file format. Ligand preparation was done by assigning Gastegier charges, merging non-polar hydrogen's, and saving in PDBQT file format using AutoDock Tools (ADT) 1.5.4.[51] X-ray crystal structure for DNA (PDB ID: 1BNA) was obtained from the Protein Data Bank (http://www.rcsb.org/pdb). Gastegier charges were assigned to DNA and saved in PDBQT file format using ADT. Preparation of parameter files for grid and docking was done using ADT. Docking was performed with AutoDock 4.0 (Scripps Research Institute, USA) considering all the rotatable bonds of ligand as rotatable and DNA as rigid.[52] The grid centre was established by centring the grid box on whole DNA. Grid box size of $60 \times 80 \times 110$ Å with 0.375 Å spacing was used. Macromolecule docking was performed using an empirical-free energy function and Lamarckian Genetic Algorithm, with an initial population of 150 randomly placed individuals, a maximum number of 2,500,000 energy evaluations, a mutation rate of 0.02, and crossover rate of 0.80. Fifty independent docking runs were performed

for each ligand and DNA–ligand complex for lowest free energy of binding conformation from the largest cluster, which was written and saved in PDBQT format. These PDBQT files had been converted to PDB file format. Docking results were analyzed using UCSF Chimera[53] and LigPlot for possible polar and hydrophobic interactions.[54]

5. Conclusions

Anticancer potential of curcumin-I (natural product) was exploited by synthesizing its Knoevenagel's condensates and their Schiff's bases. In total, 12 compounds were synthesized (**4a–6d**), purified and characterized. The reported compounds were less hemolytic than standard drug doxorubicin; an indication of safe future medication. The values of DNA binding constant (1.4×10^3–$8.1 \times 10^5\ M^{-1}$) and % cell line viability [MCF-7 (wild) 59% at1.0 μg/mL] were other signals towards their good anticancer activities. These results were due to good DNA interacting tendency of the reported compounds. The determination of mechanism of action at supra-molecular level showed that small molecular size compounds (**4a–d**) interacted with DNA through minor grooves. On the other hand, medium (**5a–d**) and large molecular size (**6a–d**) compounds interacted with DNA through major grooves. The occurrence of hyper- and hypo-chromism was an indication of binding of these compounds with DNA through both intercalation and electrostatic attractions. These results were also supported by the docking studies. The docking energies varied from −7.30 to −13.4 kcal/mol with 1–6 hydrogen bonds. A critical evaluation of all the properties of the reported compounds indicated their quite bright future as anticancer candidates.

Acknowledgment

The authors are thankful to CSIR (Council of Scientific and Industrial Research), New Delhi for providing Senior Research Fellowship to Ashanul Haque.

Supplementary data

Supplementary data associated with this article can be found, in the online version, at http://dx.doi.org/10.1016/j.bmc.2013.04.018.

References and notes

1. World Health Statistics 2012. World Health Organization: Geneva, 2012.
2. American Cancer Society *Cancer Facts & Figures 2012*; American Cancer Society: Atlanta, 2012.
3. Dikshit, R.; Gupta, P. C.; Ramasundarahettige, C.; Gajalakshmi, V.; Aleksandrowicz, L.; Badwe, R.; Kumar, R.; Roy, S.; Suraweera, W.; Bray, F.; Mallath, M.; Singh, P. K.; Sinha, D. N.; Shet, A. S.; Gelband, H.; Jha, P. *Lancet* **1807**, *2012*, 379.
4. Isakoff, S. *Cancer J.* **2010**, *16*, 53.
5. Newman, D. J.; Cragg, G. M. J. *Nat. Prod.* **2012**, *75*, 311.
6. Vasilevich, N. I.; Kombarov, R. V.; Genis, D. V.; Kirpichenok, M. A. *J. Med. Chem.* **2012**, *55*, 7003.
7. Ali, I.; Rahisuddin, Saleem K.; Haque, A.; El-Azzouny, A. *Egypt. Pharm. J.* **2010**, *9*, 133.
8. Lee, K. H.; Ab Aziz, F. H.; Syahida, A.; Abas, F.; Shaari, K.; Israf, D. A.; Lajis, N. H. *Eur. J. Med. Chem.* **2009**, *44*, 3195.
9. Venkatesan, P.; Rao, M. N. *J. Pharm. Pharmacol.* **2000**, *52*, 1123.
10. Aggarwal, B. B.; Kumar, A.; Bharti, A. C. *Anticancer Res.* **2003**, *23*, 363.
11. Amolins, M. W.; Peterson, L. B.; Blagg, B. S. *Bioorg. Med. Chem.* **2009**, *17*, 360.
12. Padhye, S.; Chavan, D.; Pandey, S.; Deshpande, J.; Swamy, K. V.; Sarkar, F. H. *Mini-Rev. Med. Chem.* **2010**, *10*, 372.
13. Sahu, P. K.; Sahu, P. K.; Gupta, S. K.; Thavaselvam, D.; Agarwal, D. D. *Eur. J. Med. Chem.* **2012**, *54*, 366.
14. Mishra, S.; Karmodiya, K.; Surolia, N.; Surolia, A. *Bioorg. Med. Chem.* **2008**, *16*, 2894.
15. Qiu, X.; Du, Y.; Lou, B.; Zuo, Y.; Shao, W.; Huo, Y.; Huang, J.; Yu, Y.; Zhou, B.; Du, J.; Fu, H.; Bu, X. *J. Med. Chem.* **2010**, *53*, 8260.
16. Simoni, D.; Rizzi, M.; Rondanin, R.; Baruchello, R.; Marchetti, P.; Invidiata, F. P.; Labbozzetta, M.; Poma, P.; Carina, V.; Notarbartolo, M.; Alaimo, A.; Alessandro, N. D. *Bioorg. Med. Chem. Lett.* **2008**, *18*, 845.
17. Ali, I.; Saleem, K.; Wesselinova, D.; Haque, A. *Med. Chem. Res.* **2013**, *22*, 1386.
18. Howard, S.; Berdini, V.; Boulstridge, J. A.; Carr, M. G.; Cross, D. M.; Curry, J.; Devine, L. A.; Early, T. R.; Fazal, L.; Gill, A. L.; Heathcote, M.; Maman, S.; Matthews, J. A.; McMenamin, R. L.; Navarro, E. F.; O'Brien, M. A.; O'Reilly, M.; Rees, D. C.; Reule, M.; Tisi, D.; Williams, G.; Vinkovic, M.; Wyatt, P. G. *J. Med. Chem.* **2009**, *52*, 379.
19. Bekhit, A. A.; Abdel-Aziem, T. *Bioorg. Med. Chem.* **2004**, *12*, 1935.
20. Adhikari, A.; Kalluraya, B.; Sujith, K. V.; Gouthamchandra, K.; Jairam, R.; Mahmood, R. *Eur. J. Med. Chem.* **2012**, *55*, 467.
21. Nitulescu, G. M.; Draghici, C.; Missir, A. V. *Eur. J. Med. Chem.* **2010**, *45*, 4914.
22. Bouabdallah, I.; M'Barek, L.; Zyad, A.; Ramdani, A. A.; Zidane, I.; Melhaoui, A. *Nat. Prod. Res.* **2007**, *21*, 298.
23. Havrylyuk, D.; Zimenkovsky, B.; Vasylenko, O.; Zaprutko, L.; Gzella, A.; Lesyk, R. *Eur. J. Med. Chem.* **2009**, *44*, 1396.
24. Shaharyar, M.; Abdullah, M. M.; Bakht, M. A.; Majeed, J. *Eur. J. Med. Chem.* **2010**, *45*, 114.
25. Situ, H.; Bobek, L. *Antimicrob. Agents Chemother.* **2000**, *44*, 1485.
26. Christie, M. S.; Kenneth, L. R.; David, B. W. *Toxicol. Sci.* **2007**, *97*, 163.
27. Barton, J. K.; Danishefsky, A.; Goldberg, J. *J. Am. Chem. Soc.* **1984**, *106*, 2172.
28. Shahabadi, N.; Kashanian, S.; Purfoulad, M. *Spectrochim. Acta, Part A* **2009**, *72*, 757.
29. Liu, X. W.; Li, J.; Deng, H.; Zheng, K. C.; Mao, Z. W.; Ji, L. N. *Inorg. Chim. Acta* **2005**, *358*, 3311.
30. Liu, X. W.; Li, J.; Li, H.; Zheng, K. C.; Chao, H.; Ji, L. N. *J. Inorg. Biochem.* **2005**, *99*, 2372.
31. Liu, J. G.; Zhang, Q. L.; Shi, X. F.; Ji, L. N. *Inorg. Chem.* **2001**, *40*, 5045.
32. Pyle, A. M.; Rehmann, J. P.; Meshoyrer, R.; Kumar, C. V.; Turro, N. J.; Barton, J. K. *J. Am. Chem. Soc.* **1989**, *111*, 3051.
33. Indumathy, R.; Kanthimathi, M.; Weyhermuller, T.; Nair, B. U. *Polyhedron* **2008**, *27*, 3443.
34. Allardyce, C. S.; Dyson, P. J.; Ellis, D. J.; Heath, S. L. *Chem. Commun.* **2001**, 1396.
35. Pasternack, R. F.; Gibbs, E. J.; Villafrancas, J. *J. Biochem.* **1983**, *22*, 2406.
36. Zhao, P.; Xu, L.; Huang, J.; Liu, J.; Yu, H.; Zheng, K.; Ji, L. *Spectrochim. Acta, Part A: Mol. Biomol. Spectrosc.* **2008**, *71*, 1216.
37. Guo, H.; Cai, C.; Gong, H.; Chen, X. *Spectrochim. Acta, Part A: Mol. Biomol. Spectrosc.* **2011**, *79*, 92.
38. Psomas, G.; Tarushi, A.; Efthimiadou, E. K. *Polyhedron* **2008**, *27*, 133.
39. Chen, L. M.; Liu, J.; Chen, J. C.; Tan, C. P.; Shi, S.; Zheng, K. C.; Ji, L. N. *J. Inorg. Biochem.* **2008**, *102*, 330.
40. Pratviel, G.; Bernadou, J.; Meunier, B. *Adv. Inorg. Chem.* **1998**, *45*, 251.
41. Arjmand, F.; Parveen, S.; Afzal, M.; Toupet, L.; Ben Hadda, T. *Eur. J. Med. Chem.* **2012**, *49*, 141.
42. Haq, I. *Arch. Biochem. Biophys.* **2002**, *403*, 1.
43. Sun, Y.; Zhang, H.; Bi, S.; Zhouf, X.; Wang, L.; Yan, Y. *J. Lumin.* **2011**, *131*, 2299.
44. Bayomi, S. M.; El-Kashef, H. A.; El-Ashmawy, M. B.; Nasr, M. N. A.; El-Sherbeny, M. A.; Badria, F. A.; Abou-zeid, L. A.; Ghaly, M. A.; Abdel-Aziz, N. I. *Med. Chem. Res.* **2013**, *22*, 1147.
45. Neidle, S. *Nat. Prod. Rep.* **2001**, *18*, 291.
46. Hamilton, P. L.; Arya, D. P. *Nat. Prod. Rep.* **2012**, *29*, 134.
47. Péret-Almeida, L.; Cherubino, A. P. F.; Alves, R. J.; Dufossé, L.; Gloria, M. B. A. *Food Res. Int.* **2005**, *38*, 1039.
48. ASTM F756-00 *Standard Practice for Assessment of Hemolytic Properties of Materials*; ASTM International: West Conshohocken, PA, USA, 2000. http://dx.doi.org/10.1520/F0756-00.
49. Wolfe, A.; Shimer, G. H., Jr.; Meehan, T. *Biochemistry* **1987**, *26*, 6392.
50. Mosman, T. *J. Immunol. Methods* **1983**, *65*, 55.
51. Sanner, M. F. *J. Mol. Graph Model* **1999**, *17*, 57.
52. Morris, G. M.; Goodsell, G. S.; Halliday, R. S.; Huey, R.; Hart, W. E.; Belew, R. K.; Olson, A. J. *J. Comput. Chem.* **1998**, *19*, 1639.
53. Pettersen, E. F.; Goddard, T. D.; Huang, C. C.; Couch, G. S.; Greenblatt, D. M.; Meng, E. C.; Ferrin, T. E. *J. Comput. Chem.* **2004**, *25*, 1605.
54. Laskowski, R. A.; Swindells, M. B. *J. Chem. Inf. Model.* **2011**, *51*, 2778.